

Modeling and Performance Analysis in Cache-enabled Millimeter Wave HetNets with Access and Backhaul Integration

Hao Wu, Chenwu Zhang, Hancheng Lu, *Member, IEEE*, Qi Hu

Index Terms

Millimeter Wave; Heterogeneous Networks; Caching; Area Spectral Efficiency

I. INTRODUCTION

Recently, mmWave-based access and backhaul integration heterogeneous cellular networks (mABHetNets) has been envisioned in 5G dense cellular networks to satisfy the rapidly growing traffic demand [1]–[4]. In the mABHetNets, high-power mmWave MBSs are overlaid by denser lower-power mmWave SBSs where MBSs and SBSs provide high rate service to the users by wireless access link while the MBS maintains the backhaul capacity of the SBSs by the wireless backhaul link. Both the access link and the backhaul link share the same mmWave spectrum resources, which is called a mmWave-based access and backhaul integration architecture. Average potential throughput (APT) and area spectral efficiency (ASE) have become the two major performance metrics for 5G dense cellular networks [5]–[10]. APT focuses on analyzing user's average throughput with the specific rate requirement [5]. [6] analyze APT of different user's SINR requirements in a new path loss model. Further, [7] investigates APT of user in line-of-sight (LOS) and non-line-of-sight (NLOS) scenarios respectively. Besides, another widely used metric ASE is defined as the spectral efficiency per unit area of cellular networks [8]. [9] discussed

Hao Wu, Chenwu Zhang and Hancheng Lu are with CAS Key Laboratory of Wireless Optical Communication, University of Science of China, Hefei 230027, China. (Email: hwu2014@mail.ustc.edu.cn, cwzhang@mail.ustc.edu.cn, hclu@ustc.edu.cn).

Qi Hu is with University of Science and Technology of China, Hefei 230027, China. (Email: hq1998@mail.ustc.edu.cn).

the ASE in the different SBS antenna gain patterns. [10] analyzes ASE under different user association strategies in D2D millimeter-wave networks.

In mABHetNets, mmWave spectrum bandwidth partition between access link and backhaul link has played an important role in APT and ASE [11]–[13]. Since partitioned spectrum bandwidth between the access and backhaul is orthogonal, the interference between the access and backhaul is avoided and the wireless rate is improved. As the user’s data rate is influenced by both access link rate and backhaul link rate, [11] explores the optimal partition of access and backhaul bandwidth to maximize the rate coverage. In a mmWave unified access and backhaul network, [12] leverages allocated resource ratio between radio access and backhaul to study maximization of network capacity by considering the fairness among SBSs. [13] jointly studies the beamforming and bandwidth partition to improve the network capacity of mABHetNets. However, since the backhaul link may suffer relatively high path loss, a large amount of mmWave spectrum is occupied by the backhaul link to maintain the backhaul link capacity. According to the findings in [13], up to 50% mmWave spectrum will be used in backhaul link to satisfy the high speed data traffic. Such stubborn “*spectrum occupation*” in mABHetNets has restricted network performance such as ASE and APT to achieve a better possible improvement.

Nowadays, enabling caching at the wireless edge such as SBSs called cache-enabled mABHetNets has been considered as a promising way to improve the network performance [14]–[17]. Statistical reports have shown that a few popular files requested by many users account for most of the backhaul traffic load [14], [15]. Based on this fact, equipping caches at all BSs for caching the most popular contents becomes an effective method to offload the data traffic of backhaul [17]. In detail, popular files can be proactively cached at SBSs during off-peak time, and delivered to users when requested, which can significantly alleviate backhaul traffic pressure. By exploiting these benefits, equipping caches in the mABHetNets brings an opportunity to overcome *spectrum occupation* problem. When the backhaul traffic is offloaded by caching popular files at the cache of SBSs, the part of mmWave spectrum in backhaul can be transferred to the access link. With more cache capacity, more spectrum is used for the access link, both ASE and APT can be increased.

However, as we know that, additional caches will consume the power of BSs [18], [19]. Both [19] and [18] think the caching energy consumption is the key part of the total power consumption. Since BSs has a limited energy resource, when the caching power consumption is introduced, the transmission power is reduced, which will lower the data rate. Therefore, in this

paper, we attempt to explore the impact of caches on the network performance of cache-enabled mABHetNets, especially in terms of APT and ASE. We also identify the impacts of some other cache-related factors. We first derive the basic SINR distribution of the mABHetNets. Then, we further study the APT and ASE in the cache-enabled mABHetNets. To the best of our knowledge, there is no theoretical research that investigates the performance of the mABHetNets when caches are involved. Motivated by such fact, we carry out the analytical study for the cache-enabled mABHetNets. The major contributions of this paper are summarized as follows.

- We develop a tractable analytical framework by stochastic geometry tool to study the cache-enabled mABHetNets. Considering the LoS and NLoS transmission in mmWave, we derive the expression of APT and ASE where the key factors (e.g. cache capacity, bandwidth partition ratio etc.) are identified.
- With the derived performance expressions, we analyze APT and ASE over the cache capacity and bandwidth partition. In order to make the ASE expressions more tractable, we derive ASE in the special case(e.g., the noise-limited and the interference-limited case).
- We find that there exists case the optimal cache capacity. With the small cache capacity, and the corresponding APT and ASE are improved. However, when the cache capacity is larger, both APT and ASE will be decreased. With the optimal cache capacity, the optimal usage ratio of mmWave spectrum for access can be improved from 0.5 to 0.8. Besides, we also see that, some other caching parameters have a significant influence on the network performance.

Finally, extensive numerical and simulations results are carried out to validate the motivation and effectiveness of our work.

The rest of the paper is organized as follows: Sect. II gives an overview of the system model. The SINR distribution of cache-enabled mABHetNets are derived in Sec. III. Then, APT and ASE are further analyzed in Sec. IV, respectively. Last, the numerical results are presented in Section V. Finally, we conclude the paper in Section VI.

II. SYSTEM MODEL

In this section, we consider a downlink mABHetNets consisting MBS tier and SBS tier. By the stochastic geometry tool, the location of the BSs and users are described. Then, file caching model and the SINR model are illustrated. Last, the bandwidth partition between the access and backhaul link is introduced.

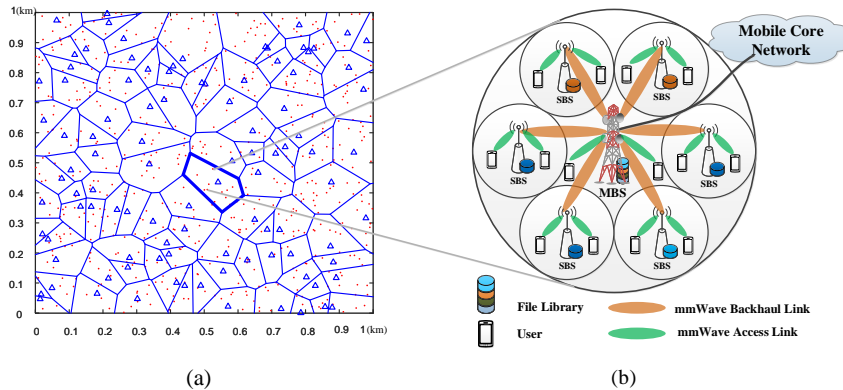


Fig. 1: (a) Example of downlink mABHetNets with two tiers of BSs: MBSs (blue triangle) are overlaid with denser SBSs (red point) (b) a megascopic cache-enabled mABHetNets

A. Network Model

In this paper, with the aid of stochastic geometry approach, a tractable analytical network model is proposed for characterizing the performance of our mABHetNets. As it is shown in Fig. 1, downlink communication in a two-tier mABHetNets is considered. The first tier of mABHetNets consist of lower-power SBSs while the second tier consists of higher-power MBSs. The MBSs is connected to the mobile core network by high-capacity optical fiber links. Besides, the MBSs provide wireless backhaul connections to the SBSs via broad mmWave spectrum. The locations of the MBSs and SBSs are assumed to follow independent Poisson point processes (PPPs), which are denoted by $\Phi_m \in \mathbb{R}_2$ and $\Phi_s \in \mathbb{R}_2$ with densities and λ_m and λ_s , respectively. Both MBSs and SBSs provide the access service to the users, which is also modeled according to independent homogeneous PPPs $\Phi \in \mathbb{R}_2$ with density λ . λ is assumed to be sufficiently larger than λ_m and λ_s so that each BS has at least one associated UE in its coverage area. The access link is also using mmWave spectrum. The above model where the nodes are distributed using PPPs has been shown to be quite effective for system-level performance evaluation of cellular networks [20].

B. Caching Model

The file library is denoted by \mathcal{F} and there are $|\mathcal{F}| = F$ files in the library. It is assumed that each file has the equal size [21] for mathematical tractability and notational simplicity. Note that when the file sizes are different from each other, such assumption can still hold since those

TABLE I: Main Symbols

Symbol	Meaning
W, W_{ac}, W_{bh}	Total spectrum bandwidth, access link bandwidth and backhaul link bandwidth
η	mmWave bandwidth partition ratio for access link
α_L, α_{NL}	Path loss exponent in LoS and NLoS transmission
$\lambda_s, \lambda_m, \lambda$	Density of MBS, SBS and user, respectively
C	Cache capacity of a SBS
F	Number of files
p_h	Cache hit ratio of a SBS
P_m^{tot}, P_s^{tot}	Total power of an MBS and an SBS, respectively
P_m^{tr}, P_s^{tr}	Transmission power of an MBS and an SBS, respectively
B_m, B_s	The association bias factor of MBS and SBS
w_{ca}	Caching power consumption coefficient

files can be divided into chunks of equal size. Different files have different popularities. The file popularity distribution changes with time slowly so that it can be regarded as static [22]. Then, based on collected statistical information and the machine learning algorithm, the file popularity can often be predicted [23]. Zipf distribution is widely used to model the popularity of file f , $\forall f \in \{1, \dots, F\}$: the probability of the f -th file is $p_f = \frac{f^{-\gamma_p}}{\sum_{g=1}^F g^{-\gamma_p}}$, where γ_p is the Zipf exponent reflecting different levels of skewness of the distribution [24], [25]. The typical value of γ_p is between 0.5 and 1.0, where higher value causes more ‘‘peakiness’’ of the distribution [25].

For the cache-enabled MBS and SBS, the cache capacity of the SBS and MBS are denoted by F and C (file units), respectively. As each MBS is often equipped with large cache capacity, we assume that the MBS can cache the total file library [26]. In this paper, the most popular caching strategy is applied for each BS : each BS caches the most popular contents until its storage is full [17]. Hence, the cache hit ratio of a SBS can be calculated as

$$p_h = \frac{\sum_{f=1}^C f^{-\gamma_p}}{\sum_{g=1}^F g^{-\gamma_p}}. \quad (1)$$

C. Wireless Transmission Model

The mmWave based wireless link can be either line of sight (LOS) or non-line of sight (NLoS) transmission. Then, we consider the following path loss function defined in [27]:

$$L(r) = \begin{cases} A_L r^{-\alpha_L}, & \text{with LOS probability } \mathcal{P}_L(r) \\ A_{NL} r^{-\alpha_{NL}}, & \text{with NLoS probability } \mathcal{P}_{NL}(r) = 1 - \mathcal{P}_L(r), \end{cases} \quad (2)$$

together with the LoS probability $\mathcal{P}_L(r) = \min\left(\frac{18}{r}, 1\right)(1 - e^{-\beta r}) + e^{-\beta r}$ and r is the transmission distance. $\beta \geq 0$ is the parameter that captures density and size of obstacles between the transmitter and the receiver. As β increases, the size and density of obstacles increase, which results in lower probability of LoS transmission. The propagation is always in LOS condition when $r \leq 18m$. In practice, this implies that, for denser mABHetNets, the probability of LOS coverage is very close to one and some NLOS transmission could be neglected.

By involving the cache power consumption, we give the power model of one MBS and one SBS as follows [18]: $\rho_m P_m^{tr} + P_m^{fc} + P_m^{ca} = \rho_m P_m^{tr} + P_m^{fc} + w_{ca}F$, $\rho_s P_s^{tr} + P_s^{fc} + P_s^{ca} = \rho_s P_s^{tr} + P_s^{fc} + w_{ca}C$ where P_m^{tr} and P_s^{tr} denote transmit powers consumed at a MBS and a SBS, respectively. $\rho_m(\rho_s)$ reflects the impact of power amplifier and cooling on transmit power. $P_m^{fc}(P_s^{fc})$ is the fixed circuits-related power consumption at a BS. $P_m^{ca}(P_s^{ca})$ is the power consumption for caching files at a BS. Usually, $P_m^{fc}(P_s^{fc})$ is assumed to be a fixed power consumption constant [28]. To quantify power consumption for caching, we adopt a power-proportional model, which is widely used in cache enabled radio access network [18], [19]. In the power-proportional model, the caching power consumption is proportional to the cache capacity. Then, the caching power consumption of the MBS and SBS are given as follows: $P_m^{ca} = w_{ca}F$, $P_s^{ca} = w_{ca}C$, where w_{ca} is the power coefficient of cache hardware in watt/bit. F is the total size of all the files. Here, we assume that the cache storage of the MBS is large enough and the library of all files are cached in MBS [26]. C is the cache storage of a SBS in file unit.

For each SBS, since the total power consumption P_s^{tot} is usually given, we can get $P_s^{tr} = \frac{P_s^{tot} - P_s^{fc} - w_{ca}C}{\rho_s} = P_s' - w_{ca}'C$, where $P_s' = \frac{P_s^{tot} - P_s^{fc}}{\rho_s}$ and $w_{ca}' = \frac{w_{ca}}{\rho_s}$. Here, we assume that the MBS has a large cache capacity and contains all the files in the file library. The total power consumption of a MBS is P_m^{tot} . Then the $P_m^{tr} = \frac{P_m^{tot} - P_m^{fc} - w_{ca}C}{\rho_m} = P_m' - w_{ca}^m F$ is fixed where $P_m' = \frac{P_m^{tot} - P_m^{fc}}{\rho_m}$ and $w_{ca}^m = \frac{w_{ca}}{\rho_m}$. Note that considering the total power consumption, the maximum cache capacity is $\frac{P_s^{tot}}{w_{ca}}$.

The analysis in this paper is done for the user located at the origin referred to as the typical user. Therefore, the signal-to-interference-plus-noise ratio (SINR) of a typical user at a random distance r from its associated SBS and MBS are

$$\text{SINR}_s(r) = \frac{P_s^{tr} B_s h_s L(r)}{I_s + I_m + N_0} = \frac{(P_s' - w_{ca}'C) B_s h_s L(r_s)}{\sum_{i \in \Phi_s \setminus b_{s,0}} (P_s' - w_{ca}'C) B_s h_{s,i} L(r_{s,i}) + \sum_{l \in \Phi_m} P_m^{tr} B_m h_{m,l} L(r_{m,l}) + N_0} \quad (3)$$

$$\text{SINR}_m(r) = \frac{P_m^{tr} B_m h_m L(r_m)}{I_s + I_m + N_0} = \frac{P_m^{tr} B_m h_m L(r_m)}{\sum_{i \in \Phi_s} (P_s' - w_{ca}'C) B_s h_{s,i} L(r_{s,i}) + \sum_{l \in \Phi_m \setminus b_{m,0}} P_m^{tr} B_m h_{m,l} L(r_{m,l}) + N_0} \quad (4)$$

where B_s, B_m are the association bias factor of SBS and MBS. h_s, h_m are the small-scale fadings from SBS and MBS. $L(r_m), L(r_s)$ are the path losses from the serving SBS or MBS to the typical user. r_s (r_m) is the distance between the association SBS $b_{s,0}$ (association MBS $b_{m,0}$) and the typical user. $r_{s,i}(r_{m,l})$ is the distance between the i -th SBS(l -th MBS)and the typical user. N_0 is the additive white Gaussian noise component.

To backhaul the data traffic of the SBSs, the MBS provides the wireless backhaul link. For a typical SBS that a random distance r_{bh} from its associated MBS, the SINR of the signal from the MBS to the SBS in downlink backhaul is then given as,

$$\text{SINR}_{bh}(r_{bh}) = \frac{P_m^{tr} B_m h_m L(r_{bh})}{I_{bh} + N_0} = \frac{P_m^{tr} B_m h_m L(r_{bh})}{\sum_{i \in \Phi_m \setminus b_{m,0}} P_m^{tr} B_m h_{m,i} L(r_{bh,i}) + N_0} \quad (5)$$

D. Bandwidth Partition Model

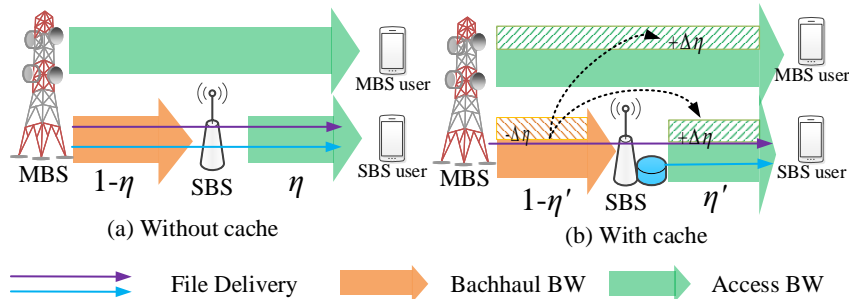


Fig. 2: Bandwidth partition between access and backhaul (a) original and (b)with cache

In this paper, we focus on the downlink data transmission using the mmWave spectrum. In Fig.2, both the access link and backhaul link use the mmWave spectrum. To avoid the interference between the access and backhaul link, the access and backhaul use orthogonal spectrum resources. The total mmWave bandwidth W for downlink transmission is partitioned into two parts: $W_{ac} = \eta W$ for access and $W_{bh} = (1 - \eta)W$ for backhaul. $\eta \in [0, 1]$ is access-backhaul bandwidth partition ratio and denotes the part of spectrum for access link. The file delivery is both related with the access link and backhaul link. Then by changing the partition ratio, both the access rate and backhaul rate in the same transmission path can maintain an effective transmission. When the cache is introduced, cached files can directly delivered from SBS and the backhaul traffic can be saved. Thus, part mmWave spectrum resource in backhaul link can be shifted to access link and the data rate is improved.

III. SINR DISTRIBUTION OF MABHETNETS

In this section, we derive the expression of SINR distribution of the typical user conditioned on its association selections and later decondition over them. As users may be covered either by the SBS or MBS, we first derive the PDF of the distance between the user and the serving SBS and MBS. Further, SINR distributions of the users associated with the serving SBS and the serving MBS are obtained. Besides, the SINR coverage probability of the SBS covered by the MBS is also obtained.

A. The PDF of Distance to Nearest Base Station

First of all, we need to derive the probability distribution function (PDF) of the distance between the typical user and its nearest BS. We focus on the typical user at the origin. When the typical user communicates with the closest BS at a distance r , no other BS can be closer than r . In other words, all interfering BSs must be farther than r . Since the typical user is associated with the closest BS via either LoS or NLoS channel, we derive these PDFs in following Lemma, respectively

Lemma 1. *The PDF of r (the distance between the typical user and the nearest SBS or MBS via a LoS/NLoS path) is written as*

$$f_{R_k}^L(r) = \mathcal{P}_L(r) \times \exp(-\pi r^2 \lambda_k) \times 2\pi r \lambda_k, \quad (6)$$

$$f_{R_k}^{NL}(r) = \mathcal{P}_{NL}(r) \times \exp(-\pi r^2 \lambda_k) \times 2\pi r \lambda_k, \quad (7)$$

where $k \in \{s, m\}$ denotes the index of SBS tier or MBS tier.

Proof. The detailed proof procedure can be found in Appendix VI-A. □

Remark 1. *The uncached file data will be delivered from the MBS to the SBS by the mmWave based wireless backhaul. Similar to the above analysis in Lemma 1, the PDFs of distance r (between the SBS and the associated the nearest MBS via a LoS/NLoS path) are*

$$f_{R_{bh}}^L(r) = \mathcal{P}_L(r) \times \exp(-\pi r^2 \lambda_m) \times 2\pi r \lambda_m \quad (8)$$

$$f_{R_{bh}}^{NL}(r) = \mathcal{P}_{NL}(r) \times \exp(-\pi r^2 \lambda_m) \times 2\pi r \lambda_m \quad (9)$$

B. Association Probability

In mABHetNets, due to the different transmission path (i.e., LoS and NLoS) and the densities of the SBS and MBS, we need to analyze the probability that a user is associated with SBS tier or with MBS tier. Besides, since in the SBS backhaul association, SBS may be associated with MBS via different transmission paths, different SBS backhaul association probabilities should be derived.

1) *user association probability*: We consider a user association based on maximum biased received power, where a mobile user is associated with the strongest BS in terms of the received power at the user. Then, for a typical user associated with the SBS tier via LoS path and NLoS path, the received powers are $P_s^{tr} B_s h_s A_L r^{-\alpha_L}$ and $P_s^{tr} B_s h_s A_{NL} r^{-\alpha_{NL}}$, respectively. For a typical user associated with the MBS tier via LoS path and NLoS path, the received powers are $P_m^{tr} B_m h_m A_L r^{-\alpha_L}$ and $P_m^{tr} B_m h_m A_{NL} r^{-\alpha_{NL}}$, respectively.

Based on the maximum biased received power association strategy, each tiers BS density and transmit power as well as transmission path determine the probability that a typical user is associated with a tier. The following lemma provides the per-tier association probability via LoS and NLoS path respectively.

Lemma 2. *For the given distance r , the probabilities that a typical user is associated with the SBS tier by LoS link and NLoS link are*

$$F_s^L(r) = p_{ln}^{ss}(r) p_{il}^{sm}(r) p_{ln}^{sm}(r) f_{R_s}^L(r), \quad (10)$$

$$F_s^{NL}(r) = p_{nl}^{ss}(r) p_{nl}^{sm}(r) p_{nn}^{sm}(r) f_{R_s}^{NL}(r) \quad (11)$$

Then, the probabilities that a typical user is associated with the MBS tier by LoS link and NLoS link are

$$F_m^L(r) = p_{ln}^{mm}(r) p_{il}^{ms}(r) p_{ln}^{ms}(r) f_{R_m}^L(r), \quad (12)$$

$$F_m^{NL}(r) = p_{nl}^{mm}(r) p_{nl}^{ms}(r) p_{nn}^{ms}(r) f_{R_m}^{NL}(r) \quad (13)$$

where $p_{ln}^{ss}(r)$ denotes the probability of the event that the user obtains the desired LoS signal from SBS tier and the NLoS interference from the SBS tier. The other probabilities have the similar definitions and can be found in the proof.

Proof. The detailed proof procedure can be found in Appendix VI-B. □

2) *SBS backhaul association probability*: The SBS will be associated with the MBS by the wireless backhaul link. The SBS backhaul association strategy is also based on the maximum biased received power from the MBS. Since the backhaul transmission includes LoS link and NLoS link, there exist two backhaul association probabilities. Similar to Lemma 2, the probabilities are as follows.

Remark 2. *Similar to Lemma 2, the probabilities that a typical SBS is associated with the MBS tier by LoS link and NLoS link are*

$$F_{bh}^L(r) = p_{ln}^{bh}(r) f_{R_bh}^L(r), \quad (14)$$

$$F_{bh}^{NL}(r) = p_{nl}^{bh}(r) f_{R_bh}^{NL}(r), \quad (15)$$

where $p_{ln}^{bh}(r)$ is the probability that the SBS is associated with the LoS MBS and the interference is from NLoS MBS. $p_{nl}^{bh}(r)$ is the probability that the SBS is associated with the NLoS MBS and the interference is from LoS MBS. $p_{ln}^{bh}(r)$ and $p_{nl}^{bh}(r)$ can be found in Appendix VI-B.

C. SINR Distribution

To study the APT and ASE performance of mABHetNets, we need first investigate the SINR distribution of the user covered by SBS/MBS tier via access link or the SINR distribution of the SBS covered by MBS via backhaul link. This SINR distribution is defined as the SINR coverage probability that the received SINR is above a pre-designated threshold γ :

$$P^{cov}(\gamma) = \Pr[\text{SINR} > \gamma] \quad (16)$$

Since the user is covered either by SBS tier or by MBS tier, we first give the two SINR distributions. Then we give the SINR distribution of the typical SBS when it is covered by MBS.

Proposition 1. *1) SINR coverage probabilities of user covered by SBS tier and MBS tier:*

The SINR coverage probability that the user is associated with the SBS or MBS is

$$\mathbb{P}_k^{cov}(\gamma) = P_{k,L}^{cov}(\gamma) + P_{k,NL}^{cov}(\gamma) \quad (17)$$

$$P_{k,L}^{cov}(\gamma) = \int_0^\infty \exp\left(\frac{-\gamma N_0}{P_k^{tr} B_k A_L r^{-\alpha_L}}\right) \mathcal{L}_{I_k}^L F_k^L(r) dr \quad (18)$$

$$P_{k,NL}^{cov}(\gamma) = \int_0^\infty \exp\left(\frac{-\gamma N_0}{P_k^{tr} B_k A_{NL} r^{-\alpha_{NL}}}\right) \mathcal{L}_{I_k}^{NL} F_k^{NL}(r) dr \quad (19)$$

where $k \in \{s, m\}$ denotes SBS or MBS, respectively. $P_{k,L}^{cov}(\gamma) = \mathbb{E}_r [\mathbb{P} [\text{SINR}_k^L(r) \geq \gamma]]$ is the probability that the user is covered by SBS or MBS with LoS based signal and $P_{k,NL}^{cov}(\gamma) = \mathbb{E}_r [\mathbb{P} [\text{SINR}_k^{NL}(r) \geq \gamma]]$ is the probability that the user is covered by SBS or MBS with NLoS based signal. γ is the threshold for successful demodulation and decoding at the receiver. Besides, $\mathcal{L}_{I_s}^L = \mathcal{L}_{I_{s,m}}^L(\gamma r^{\alpha_L})$, $\mathcal{L}_{I_s}^{NL} = \mathcal{L}_{I_{s,m}}^{NL}(\gamma r^{\alpha_{NL}})$, $\mathcal{L}_{I_m}^L = \mathcal{L}_{I'_{s,m}}^L(\gamma r^{\alpha_L})$ and $\mathcal{L}_{I_m}^{NL} = \mathcal{L}_{I'_{s,m}}^{NL}(\gamma r^{\alpha_L})$

2) SINR coverage probabilities of SBS covered by MBS:

The SINR coverage probability that the SBS is covered by the MBS via wireless backhaul is:

$$\mathbb{P}_{bh}^{cov}(\gamma) = P_{bh,L}^{cov}(\gamma) + P_{bh,NL}^{cov}(\gamma) \quad (20)$$

$$P_{bh,L}^{cov}(\gamma) = \int_0^\infty \exp\left(\frac{-\gamma N_0}{P_m^{tr} B_m A_L r^{-\alpha_L}}\right) \mathcal{L}_{I_{bh}}^L(\gamma r^{-\alpha_L}) F_{bh}^L(r) dr \quad (21)$$

$$P_{bh,NL}^{cov}(\gamma) = \int_0^\infty \exp\left(\frac{-\gamma N_0}{P_m^{tr} B_m A_{NL} r^{-\alpha_{NL}}}\right) \mathcal{L}_{I_{bh}}^{NL}(\gamma r^{-\alpha_{NL}}) F_{bh}^{NL}(r) dr \quad (22)$$

Note that, considering a more general fading model such as Nakagami does not provide any additional design insights, but it does complicate the analysis significantly. Similar to [29] in our paper, the special case of Nakagami-Rayleigh fading is considered.

Proof. The detailed proof of Proposition 1 can be found in Appendix VI-C. \square

IV. APT AND ASE OF CACHE-ENABLE MABHETNETS

APT and ASE are applied as two significant metrics to measure the network performance. The APT focuses on the average user QoS requirement in terms of data rate while ASE mainly is used to measure the average network spectral efficiency. In this section, we first derive the APT. Then, we investigate the network ASE in bps/Hz/m² and analyze it.

A. APT of Cache-enable mABHetNets

APT captures the average number of bits that can be received by the user per unit area per unit bandwidth given a pre-designated threshold γ [5]. The definition of APT is

$$\mathcal{R}(\gamma) = \lambda_k W_k \log_2(1 + \gamma) \mathbb{P}\{\text{SINR} \geq \gamma\}$$

where $\lambda_k (k = s, m)$ is the density of SBS or MBS and W_k is allocated bandwidth to the user. γ is the user's SINR requirement.

In cache-enabled mABHetNets, APT is determined by cache capacity, bandwidth partition and SINR threshold. Then we let APT of cache-enabled mABHetNets denoted by

$$\mathcal{R}(\eta, C, \gamma_0) = \mathcal{R}_s(\eta, C, \gamma_0) + \mathcal{R}_m(\eta, \gamma_0) \quad (23)$$

where \mathcal{R}_s and \mathcal{R}_m are APT of the SBS tier and MBS tier. C is the cache capacity of SBS. η is the bandwidth partition between the access link and the backhaul link. γ_0 is the SINR threshold to guarantee the user throughput requirement. The following corollaries will give the detailed APT expression.

1) *APT of SBS tier:* For a user associated with a SBS, the transmission path include the access link between SBS and user and the backhaul link between the SBS and MBS. Besides, in cache-enabled mABHetNets, the caches in SBS tier also influence the file delivery in the transmission path. When the files are cached at the SBS, then the files can be delivered to user directly. At this time, the wireless backhaul between the SBS and the MBS will not be used. Otherwise, the uncached files will be delivered through the wireless backhaul link. Given the caches in SBS, we first give APT of SBS tier.

Corollary 1. *Since the transmission can be LoS or NLoS in wireless access link and wireless backhaul link for user associated with SBS tier, there are four cases in the SBS-tier throughput. Then*

$$\mathcal{R}_s(\eta, C, \gamma_0) = \mathcal{R}_s^{ll} + \mathcal{R}_s^{ln} + \mathcal{R}_s^{nl} + \mathcal{R}_s^{nn} \quad (24)$$

where \mathcal{R}_s^{ll} , \mathcal{R}_s^{ln} , \mathcal{R}_s^{nl} and \mathcal{R}_s^{nn} denotes the network throughput when the wireless SBS link and the wireless backhaul link are both LoS, the wireless SBS link is LoS and the wireless backhaul link is NLoS, the wireless SBS link is NLoS and the wireless backhaul link is LoS and the wireless SBS link is NLoS and the wireless backhaul link is NLoS, respectively. Then $\mathcal{R}_s^{ll}(\eta, C, \gamma_0) = \min\{\lambda_s \eta W \log_2(1 + \gamma_0) P_{s,L}^{cov}(\gamma_0), \frac{1}{1-p_h} \lambda_m W (1 - \eta) \log_2(1 + \gamma_0) P_{bh,L}^{cov}(\gamma_0)\}$. Symbol $\min\{\}$ means that the minimum value between the wireless access link rate and the wireless backhaul link rate. Following the same logic, $\mathcal{R}_s^{ln} = \min\{\lambda_s \eta W \log_2(1 + \gamma_0) P_{s,L}^{cov}(\gamma_0), \frac{1}{1-p_h} \lambda_m W (1 - \eta) \log_2(1 + \gamma_0) P_{bh,L}^{cov}(\gamma_0)\}$, $\mathcal{R}_s^{nl} = \min\{\lambda_s \eta W \log_2(1 + \gamma_0) P_{s,L}^{cov}(\gamma_0), \frac{1}{1-p_h} \lambda_m W (1 - \eta) \log_2(1 + \gamma_0) P_{bh,L}^{cov}(\gamma_0)\}$, $\mathcal{R}_s^{nn} = \min\{\lambda_s \eta W \log_2(1 + \gamma_0) P_{s,L}^{cov}(\gamma_0), \frac{1}{1-p_h} \lambda_m W (1 - \eta) \log_2(1 + \gamma_0) P_{bh,L}^{cov}(\gamma_0)\}$. Note that, $p_h = p_h(C) = \frac{\sum_{f=1}^C f^{-\gamma_p}}{\sum_{g=1}^F g^{-\gamma_p}}$ is the cache hit ratio in the SBS tier. $(1 - p_h)$ reflects the probability that the files that are not cached in SBS tier will be delivered through the backhaul link. $P_{s,L}^{cov}(\gamma_0)$ and $P_{s,NL}^{cov}(\gamma_0)$ are

the SINR coverage probability that the user is associated with the SBS via LoS and NLoS path in the Proposition 1.

2) *APT of MBS tier*: Since the signal is directly transmit by MBS to user via access link, similar to Corollary 1, we can easily give the expression of APT of MBS tier.

Corollary 2. *It is easy to obtain the average throughput of the MBS tier:*

$$\mathcal{R}_m(\eta, \gamma_0) = \lambda_m \eta W \log_2(1 + \gamma_0) P_{m,L}^{cov}(\gamma_0) + \lambda_m \eta W \log_2(1 + \gamma_0) P_{m,NL}^{cov}(\gamma_0) \quad (25)$$

where $P_{m,L}^{cov}(\gamma_0)$ and $P_{m,NL}^{cov}(\gamma_0)$ are the SINR coverage probability that the user is associated with the MBS via LoS and NLoS path in the Proposition 1.

B. User Spectral Efficiency Distribution of Cache-enable mABHetNets

Before giving the ASE of mABHetNets, the user spectral efficiency should be first analyzed. For a user associated with a SBS, the transmission rate of the user is not only related with the access rate from SBS, but also with the backhaul rate from MBS. When the files are cached at the SBS, then the files can be delivered to user directly. At this time, the wireless backhaul between the SBS and the MBS will not be used. Otherwise, the uncache files will be delivered first through the wireless backhaul link then the access link. Let ρ be the required user spectral efficiency and the p_h in (1) be the file hit ratio at the SBS. Then the required wireless backhaul link spectral efficiency is $(1 - p_h)\rho$. The definition of the user spectral efficiency distribution is $\mathbb{P}[R > \rho]$. Then in the following the proposition, we give the detailed user spectral efficiency distribution of the user.

Proposition 2. *1)The spectral efficiency distribution of a user associated with an SBS: When a user is associated with a SBS and the files are cached in SBS, the cached file will be delivered directly from SBS by the wireless access link. Otherwise, the uncached file will first delivered by the MBS through the backhaul link then through the access link. Since the wireless access link and wireless backhaul link can be LoS or NLoS, then four cases will exist as follows:*

$$\text{LoS access link \& LoS backhaul link: } \mathbb{P}[R_{s,1} > \rho] = \mathbb{P}_{s,L}^{cov}(2^{\frac{\rho}{\eta}} - 1 | r_s) \cdot \mathbb{P}_{bh,L}^{cov}(2^{\frac{(1-p_h)\rho}{(1-\eta)}} - 1 | r_{bh}),$$

$$\text{LoS access link \& NLoS backhaul link: } \mathbb{P}[R_{s,2} > \rho] = \mathbb{P}_{s,L}^{cov}(2^{\frac{\rho}{\eta}} - 1 | r_s) \cdot \mathbb{P}_{bh,NL}^{cov}(2^{\frac{(1-p_h)\rho}{(1-\eta)}} - 1 | r_{bh}),$$

$$\text{NLoS access link \& LoS backhaul link: } \mathbb{P}[R_{s,3} > \rho] = \mathbb{P}_{s,NL}^{cov}(2^{\frac{\rho}{\eta}} - 1 | r_s) \cdot \mathbb{P}_{bh,L}^{cov}(2^{\frac{(1-p_h)\rho}{(1-\eta)}} - 1 | r_{bh}),$$

$$\text{NLoS access link \& NLoS backhaul link: } \mathbb{P}[R_{s,4} > \rho] = \mathbb{P}_{s,NL}^{cov}(2^{\frac{\rho}{\eta}} - 1 | r_s) \mathbb{P}_{bh,NL}^{cov}(2^{\frac{(1-p_h)\rho}{(1-\eta)}} - 1 | r_{bh}).$$

where $R_{s,1}$ denotes the spectral efficiency of the link when the wireless access link is LoS and the backhaul link is NLoS. Similarly, $R_{s,2}$, $R_{s,3}$ and $R_{s,4}$ are the other cases. The file hit ratio is $p_h = p_h(C) = \frac{\sum_{f=1}^C f^{-\gamma_p}}{\sum_{g=1}^F g^{-\gamma_p}}$. The transmission power of a SBS is $P_s^{tr} = P_s^{tr}(C) = P'_s - w'_{ca} C$, which is related with the SBS cache capacity C . Besides, $\mathbb{P}_{s,L}^{cov}(\cdot)$ and $\mathbb{P}_{s,NL}^{cov}(\cdot)$ are the SINR distributions of the SBS-user via LoS and NLoS path. $\mathbb{P}_{bh,L}^{cov}(\cdot)$ and $\mathbb{P}_{bh,NL}^{cov}(\cdot)$ are the SINR distributions of the backhaul link between the SBS and MBS via LoS and NLoS path in Proposition 1.

2) The spectral efficiency distribution of a user associated with an MBS:

$$\text{for LoS based the access link : } \mathbb{P}[R_{m,1} > \rho] = \mathbb{P}_{m,L}^{cov}(2^{\frac{\rho}{\eta}} - 1 | r_m), \quad (26)$$

$$\text{for NLoS based the access link : } \mathbb{P}[R_{m,2} > \rho] = \mathbb{P}_{m,NL}^{cov}(2^{\frac{\rho}{\eta}} - 1 | r_m), \quad (27)$$

where $\mathbb{P}_{m,L}^{cov}(\cdot)$ and $\mathbb{P}_{m,NL}^{cov}(\cdot)$ are the SINR distributions of the MBS-user via LoS and NLoS path in Proposition 1.

Proof. The proof procedure can be found in the Appendix VI-D. \square

C. ASE of Cache-enabled mABHetNets

According to the definition of the ASE in [5], ASE can be expressed as follows:

$$\begin{aligned} \mathcal{A}(\eta, C) &= \mathcal{A}_s(\eta, C) + \mathcal{A}_m(\eta) = \lambda \mathbb{E}[R_s] + \lambda \mathbb{E}[R_m] \\ &= \lambda \mathbb{E}_r \left[\int_0^\infty \mathbb{P}[R_s > \rho | r] d\rho \right] + \lambda \mathbb{E}_r \left[\int_0^\infty \mathbb{P}[R_m > \rho | r] d\rho \right] \end{aligned} \quad (28)$$

where η is the part of the spectrum allocated to the access link and C is the cache capacity of the SBS. $\mathcal{A}_s(\eta, C)$ is the ASE of SBS tier and $\mathbb{P}[R_s > \rho]$ is user's spectral efficiency distribution when the user is associated with the SBS tier. $\mathcal{A}_m(\eta)$ is the ASE of MBS tier and $\mathbb{P}[R_m > \rho]$ is the rate distribution when the user is associated with the MBS tier.

Next, we will derive the $\mathcal{A}_s(\eta, C)$ and $\mathcal{A}_m(\eta)$, respectively.

Corollary 3. *Based on the four cases of the user's spectral efficiency distribution in Proposition 2, the ASE of SBS tier is*

$$\begin{aligned} \mathcal{A}_s(\eta, C) &= \lambda \left(\int_0^\infty \int_0^\infty \left[\int_0^\infty \mathbb{P}[R_{s,1} > \rho] d\rho \right] F_s^L(r_s) F_{bh}^L(r_{bh}) \right. \\ &+ \left[\int_0^\infty \mathbb{P}[R_{s,2} > \rho] d\rho \right] F_s^L(r_s) F_{bh}^{NL}(r_{bh}) + \left[\int_0^\infty \mathbb{P}[R_{s,3} > \rho] d\rho \right] F_s^{NL}(r_s) F_{bh}^L(r_{bh}) \\ &+ \left. \left[\int_0^\infty \mathbb{P}[R_{s,4} > \rho] d\rho \right] F_s^{NL}(r_s) F_{bh}^{NL}(r_{bh}) dr_s dr_{bh} \right) \end{aligned} \quad (29)$$

where cache capacity C exists in the spectral efficiency $\mathbb{P}[R_{s,1} > \rho]$, $\mathbb{P}[R_{s,2} > \rho]$, $\mathbb{P}[R_{s,3} > \rho]$ and $\mathbb{P}[R_{s,4} > \rho]$ (proposition 2).

And ASE of MBS tier is

$$\mathcal{A}_m(\eta) = \lambda \left(\int_0^\infty \left[\int_0^\infty \mathbb{P}[R_{m,1} > \rho] d\rho \right] F_m^L(r_m) + \left[\int_0^\infty \mathbb{P}[R_{m,2} > \rho] d\rho \right] F_m^{NL}(r_m) dr_m \right) \quad (30)$$

where $\mathbb{P}[R_{m,1} > \rho] = \mathbb{P}_{m,L}^{cov}(2^{\frac{\rho}{\eta}} - 1 | r_m)$ and $\mathbb{P}[R_{m,2} > \rho] = \mathbb{P}_{m,NL}^{cov}(2^{\frac{\rho}{\eta}} - 1 | r_m)$.

Remark 3. From (28) and (29), when the file hit ratio is improved, more files can be delivered from the SBS tier to users directly and the network throughput can be increased. Therefore, ASE can be increased. On one hand, the most efficient case is the file popularity can be more centralized, which means less files own more high popularity (i.e., $p_h = p_h(C) = \frac{\sum_{f=1}^C f^{-\gamma_p}}{\sum_{g=1}^F g^{-\gamma_p}}$ has a higher γ_p). On the other hand, the cache capacity is increased to raise the hit ratio p_h . However, we can see that more power is consumed for cache and the transmission power is decreased, which decrease the ASE. All the analysis will be verified in the numerical results.

D. A Special Case: the Noise-Limited mABHetNets

Based on the research in [30]–[33], under the lower SBS density, mABHetNets will be noise-limited. In mmWave communication systems, mmWave has a high signal transmission strength in LoS links. However, when the density of SBS is lower, the number of LoS link will decrease. The LoS based interferences of the intra-tier and cross-tier can be omitted. Therefore, the noise has a more important influence on the mmWave signal transmission. According to such situation, we want to investigate the ASE in cache-enabled mABHetNets in this noise-limited case. [33].

Here, the density λ_m of MBS in a real mABHetNets is low and fixed. Therefore, in this section, the low density is referring in particular to the SBS density λ_s .

Corollary 4. The ASE of mABHetNets in the noise-limited case is

$$\mathcal{A}^{\text{Noi}}(\eta, C) = \mathcal{A}_s^{\text{Noi}}(\eta, C) + \mathcal{A}_m^{\text{Noi}}(\eta) \quad (31)$$

where $\mathcal{A}_s^{\text{Noi}}(\eta, C)$ and $\mathcal{A}_m^{\text{Noi}}(\eta)$ are the ASEs of SBS tier and MBS tier in the noise-limited case, respectively.

With $I_r = I_m = I'_r = I'_m = 0$ in the general ASE expression of SBS tier (29), ASE of SBS tier in the noise-limited mABHetNets is

$$A_s^{\text{Noi}}(\eta, C) = \lambda \left(\int_0^\infty \int_0^\infty \int_0^\infty A_1(\eta, C) F_s^{\text{L}}(r_s) F_{bh}^{\text{L}}(r_{bh}) + A_2(\eta, C) F_s^{\text{L}}(r_s) F_{bh}^{\text{NL}}(r_{bh}) \right. \\ \left. A_3(\eta, C) F_s^{\text{NL}}(r_s) F_{bh}^{\text{L}}(r_{bh}) + A_4(\eta, C) F_s^{\text{NL}}(r_s) F_{bh}^{\text{NL}}(r_{bh}) \right) d\rho dr_s dr_{bh} \quad (32)$$

where $A_1(\eta, C) = \exp\left(\frac{\frac{\rho}{P_s^{\text{tr}} B_s A_L r_s^{-\alpha_{\text{L}}}} - (2\frac{\rho}{\eta} - 1)N_0}{P_m^{\text{tr}} B_m A_L r_{bh}^{-\alpha_{\text{L}}}} + \frac{(1-p_h(C))\rho}{(1-\eta)} - 1)N_0\right)$, $A_2(\eta, C) = \exp\left(\frac{\frac{\rho}{P_s^{\text{tr}} B_s A_L r_s^{-\alpha_{\text{L}}}} - (2\frac{\rho}{\eta} - 1)N_0}{P_m^{\text{tr}} B_m A_{\text{NL}} r_{bh}^{-\alpha_{\text{NL}}}} + \frac{(1-p_h(C))\rho}{(1-\eta)} - 1)N_0\right)$,
 $A_3(\eta, C) = \exp\left(\frac{\frac{\rho}{P_s^{\text{tr}} B_s A_{\text{NL}} r_s^{-\alpha_{\text{NL}}}} - (2\frac{\rho}{\eta} - 1)N_0}{P_m^{\text{tr}} B_m A_L r_{bh}^{-\alpha_{\text{L}}}} + \frac{(1-p_h(C))\rho}{(1-\eta)} - 1)N_0\right)$, $A_4(\eta, C) = \exp\left(\frac{\frac{\rho}{P_s^{\text{tr}} B_s A_{\text{NL}} r_s^{-\alpha_{\text{NL}}}} - (2\frac{\rho}{\eta} - 1)N_0}{P_m^{\text{tr}} B_m A_{\text{NL}} r_{bh}^{-\alpha_{\text{NL}}}} + \frac{(1-p_h(C))\rho}{(1-\eta)} - 1)N_0\right)$,
 $p_h = p_h(C) = \frac{\sum_{f=1}^C f^{-\gamma_p}}{\sum_{g=1}^F g^{-\gamma_p}} P_s^{\text{tr}} = P'_s - w'_{\text{ca}} C$.

In the same way, from the general ASE expression of MBS tier in (30), the ASE of MBS tier in noise-limited environment is

$$A_m^{\text{Noi}}(\eta) = \lambda \left(\int_0^\infty \int_0^\infty \exp\left(\frac{-(2\frac{\rho}{\eta} - 1)N_0}{P_m^{\text{tr}} B_m A_L r_m^{-\alpha_{\text{L}}}}\right) F_m^{\text{L}}(r_m) + \exp\left(\frac{-(2\frac{\rho}{\eta} - 1)N_0}{P_m^{\text{tr}} B_m A_{\text{NL}} r_m^{-\alpha_{\text{NL}}}}\right) F_m^{\text{NL}}(r_m) \right) d\rho dr_m \quad (33)$$

Note that, since the density of MBS tier is low, the transmission of the MBS tier can be considered as noise-limited.

Remark 4. Based on the SINR expression in (3), (4) and (5), the SINR without interference in the noise-limited mABHetNets is larger than the original one, the approximated ASE in (31) is actually a tighter upper bound of the original ASE in (28). We show later in the numerical results that ignoring the interference in the noise-limited mABHetNets introduces a negligible error.

E. A Special Case: Interference-Limited

When the density of SBS is very high, the LoS link based desired signal and interference will become dominant [34], [35]. At this time the NLoS based signal and interference and the noise received at the typical user are usually omitted. Such cache-enabled mABHetNets is called interference-limited one. Then, in the interference-limited mABHetNets, with $N_0 = 0$ and ignored NLoS transmission in (3) and (4), ASE of SBS tier is given in below lemma. Since the interference-limited case exist in the denser SBS and not related to the MBS tier of lower density.

Proposition 3. The ASE in the interference-limited mABHetNets is

$$\mathcal{A}^{\text{Int}}(\eta, C) = \mathcal{A}_s^{\text{Int}}(\eta, C) + \mathcal{A}_m^{\text{Int}}(\eta) \quad (34)$$

where $\mathcal{A}_s^{\text{Int}}(\eta, C)$ and $\mathcal{A}_m^{\text{Int}}(\eta)$ are the ASEs of SBS tier and MBS tier in the interference-limited case, respectively.

Based on the general SBS ASE in (29), the SBS ASE in the interference-limited case is

$$\begin{aligned} \mathcal{A}_s^{\text{Int}}(\eta, C) &= \lambda \left(\int_0^\infty \int_0^\infty \int_0^\infty \bar{\mathcal{L}}_{I_{s,m}}^{\text{L,int}} \left((2^{\frac{\rho}{\eta}} - 1) r_s^{\alpha_L} \right) \mathbb{P}_{bh,L}^{\text{cov}} \left(2^{\frac{(1-p_h)\rho}{(1-\eta)}} - 1 | r_{bh} \right) F_s^{\text{L}}(r_s) F_{bh}^{\text{L}}(r_{bh}) d\rho dr_s dr_{bh} \right. \\ &+ \left. \int_0^\infty \int_0^\infty \int_0^\infty \bar{\mathcal{L}}_{I_{s,m}}^{\text{L,int}} \left((2^{\frac{\rho}{\eta}} - 1) r_s^{\alpha_L} \right) \mathbb{P}_{bh,\text{NL}}^{\text{cov}} \left(2^{\frac{(1-p_h)\rho}{(1-\eta)}} - 1 | r_{bh} \right) F_s^{\text{L}}(r_s) F_{bh}^{\text{NL}}(r_{bh}) d\rho dr_s dr_{bh} \right) \end{aligned} \quad (35)$$

where $\bar{\mathcal{L}}_{I_{s,m}}^{\text{L,int}}(\cdot)$ are the Laplace transform of the cumulative interference from the SBS tier in the interference-limited case. $\mathbb{P}_{bh,L}^{\text{cov}}(\cdot)$ and $\mathbb{P}_{bh,\text{NL}}^{\text{cov}}(\cdot)$ are the SINR distributions in (21) and (22), respectively.

It is noted that, the ASE of MBS in the interference-limited case is the same as the general expression in (30) since the MBS density is not changed. Namely,

$$\mathcal{A}_m^{\text{Int}}(\eta) = \mathcal{A}_m(\eta). \quad (36)$$

Proof. The detailed proof can be found in Appendix VI-E. □

Remark 5. Based on the SINR expression in (3), (4) and (5), SINR with no NLoS interference is larger than the original one, the approximated ASE in (34) another tighter upper bound of the original ASE in (28). We show later in the numerical results that ignoring the NLoS interference and noise in mABHetNets introduces a negligible error.

V. NUMERICAL RESULTS

In this section, we use numerical results to validate and evaluate of APT and ASE of the cache-enabled mHetNets. We further study APT and ASE under different network scenarios and cache parameters.

A. Parameter Setting

The density of the SBS λ_s and the MBS λ_m are 10^{-4} BSs/m² and 10^{-5} BSs/m². Note that the density of the users is assumed to be sufficiently larger than that of the BS so that each BS has at least one associated user in its coverage. The density of the users $\lambda_u = 3 \times 10^{-4}$ users/m². The Zipf distribution parameter γ_p of file popularity is 0.6 [24]. Based on [19], we can assume that each file unit has the same size of 4MB. The number of files in the file library is 1000

file units. The cache capacity of SBS is 100 file units. To reflect the caching power model, we adopt the caching power coefficient ω_{ca} which is 2.5×10^{-9} W/bit [18]. According to the simulation requirement, the total power of SBS and MBS is set as 9.1W and 610W to maintain the transmission power consumption and caching power consumption. Other default simulation configurations are listed in Table II, based on 3GPP specification and literatures [13], [36]–[39]. All the above settings will be changed according to different scenarios.

TABLE II: Simulation parameters

Parameters	Values
Total mmWave spectrum bandwidth W	400 MHz
LoS pathloss parameters A_L, α_L	$10^{-10.38}, 2.09$
NLoS pathloss parameters A_{NL}, α_{NL}	$10^{-14.54}, 3.75$
Noise Power N_0	5 dB
Fixed circuit power at MBS	10.16W
Fixed circuit power at SBS	0.1W
Power amplifier and cooling coefficient ρ_s and ρ_m	4, 15.13
Association biases of SBS and MBS B_s and B_m	10, 1
Blockage rate β	2.7×10^{-2}

B. APT of mABHetNets

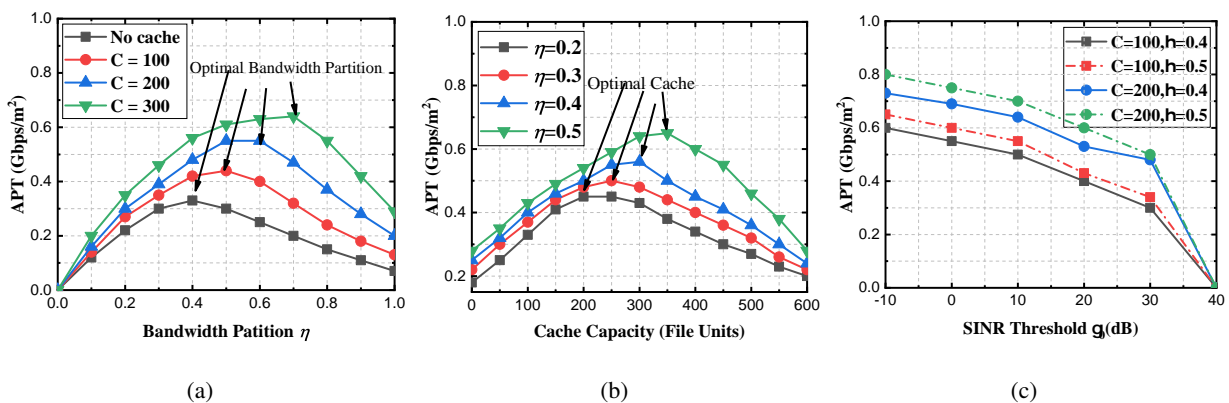


Fig. 3: APT of the mABHetNets under different (a) bandwidth partitions (γ_0 is 10dB), (b) cache capacities (γ_0 is 10dB) and (c) SINR thresholds.

To verify the APT performance in cache-enabled mHeNets, APTs under different network parameter or caching parameters are given. In Fig. 3(a), APT will increase as the bandwidth partition increases and then it decreases. That means there exist the optimal bandwidth in APT.

This is because, when the backhaul spectrum bandwidth is enough, transferring some bandwidth to the access can increase the throughput of the user. However, when more bandwidth is used in access, the backhaul link throughput cannot maintain the backhaul of the access throughput and the total throughput is reduced. In Fig. 3(b), APT also increase with the increasing cache capacity, when the backhaul throughput is limited with lower backhual bandwidth. As more cache files can improver the cache hit ratio of SBS and less files will use backhaul resource. Then more files can be obtained by access without bandwidth and the ASE is improved. However, when the cache capacity is over 600, APT is zero. Such result is because that the maximum power of SBS is limited and more cache capacity consumes more power and the transmission power is reduced. The reduced transmission power will decrease the data rate and APT. Since the APT is related to the user rate requirement, APT is shown under different SINR thresholds in Fig. 3(c). High SINR threshold will decrease APT of user. This is due to the fact that the path loss and fading make the received power lower and the received SINR lower than the threshold. However, at the same SINR threshold, more cache capacity and more bandwidth partition can cause more APT.

C. ASE Performance under bandwidth partition and Cache Capacity

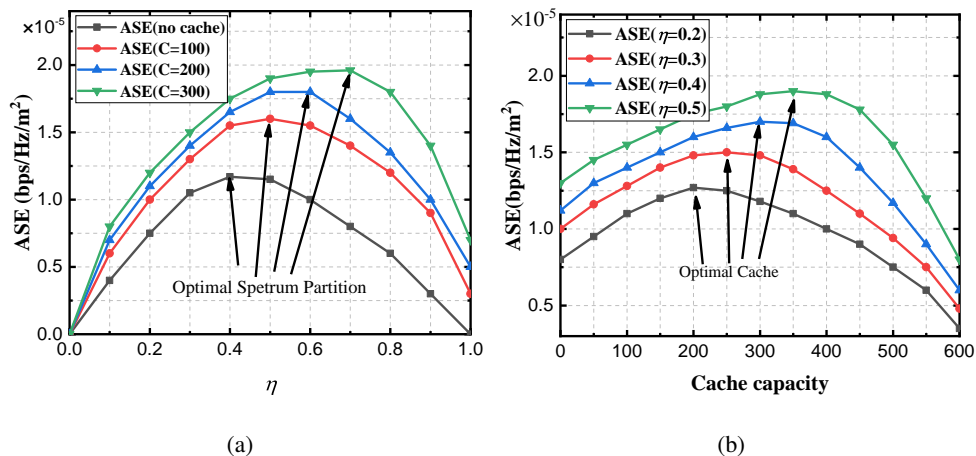


Fig. 4: ASE of the mABHetNets under different bandwidth partition (a) and file cache.

To verify the impact of the bandwidth partition on ASE, we changed the bandwidth partition η under different the cache capacity in SBS. In Fig. 4(a), we can see that, the ASE of mABHetNets first increases as the more spectrum resource is allocated to the access link including SBS and

MBS. This is because the backhaul resource is enough and can be shifted to the access backhaul to improve the ASE. However, when less spectrum is used in backhaul link, the wireless backhaul link rate becomes a bottleneck and the ASE decreases. When $C = 300$, the ASE gain of caching over not caching is about 200%. The corresponding optimal $\eta = 0.4$ is improved to 0.7 with 75% gain.

Besides, to verify the impact of the number of the cached files, we changed the cache C under different bandwidth partition Fig. 4(b). ASE can be increased when the cache capacity is increased. This is because when the backhaul bandwidth is limited, the backhaul becomes the bottleneck of the file delivery. With more cache capacity, the cache hit ratio is increased, and then more files can be sent to users directly and the impact of backhaul is reduced. However, more cache capacity consumes more power and reduce the transmission power, which reduce the ASE.

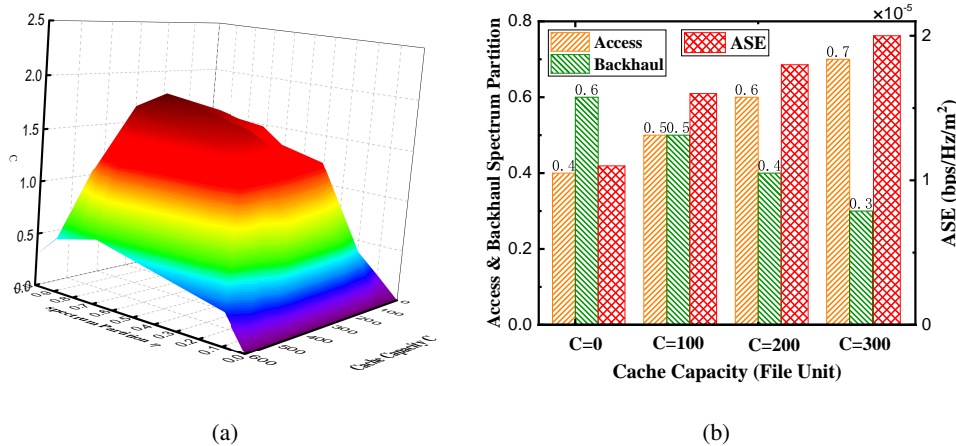


Fig. 5: The ASE of the mABHetNets with cache capacity and bandwidth partition.

To further look into the joint impacts of bandwidth partition and cache capacity on the ASE, we show the 3-dimensional numerical results of ASE in Fig. 5(a). Actually, there exist the optimal cache capacity and the optimal bandwidth. under some cases, cache capacity can improve ASE apparently. In Fig. 5(b), under the small cache capacity, more cache capacities cause more access bandwidth (over optimized bandwidth partition) and increase ASE.

D. the impact of cache on $\Delta\eta$

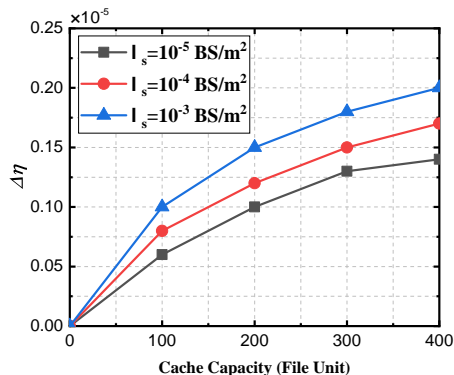


Fig. 6: Saved spectrum for access service under different cache capacities.

From the figure, when the cache capacity is larger, more bandwidth will be used in the access link compared with the uncached case in traditional mABHetNets. For a give cache capacity, by adjusting the bandwidth partition for access and backhaul link, the optimal ASE will be obtained. Compared with the traditional mABHetNets, more spectrum resource will be used for access link. From Fig. 6, we can see that, when 400 files are cached in SBS, over 20% spectrum resource is saved from the backhaul link to the access link to improve the ASE.

E. Impact of Other Key Cache Parameters on ASE

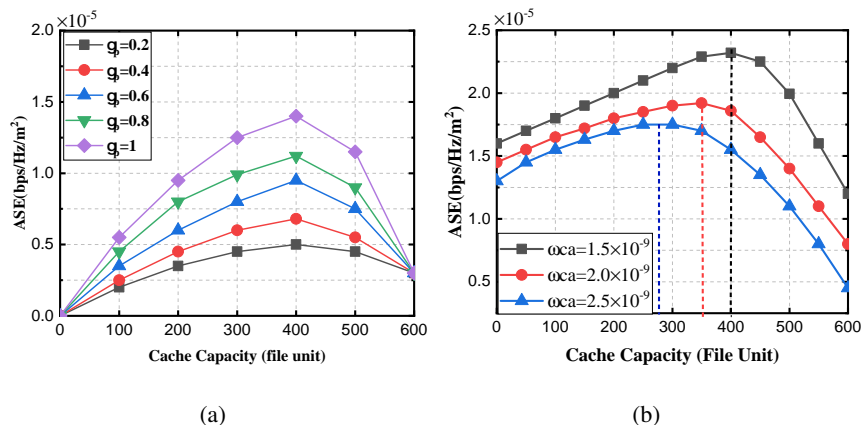


Fig. 7: Impact of cache parameter on ASE

We want to further observe the ASE of cache-enabled mABHetNets under the key cache parameters. Both the Zipf distribution parameter γ_p and the caching power coefficient ω_{ca} reflect

the characteristics of cache-enabled mABHetNets. In 7(a), we show ASE versus the cache capacity with different Zipf parameter γ_p . All the results are based on the optimal bandwidth partition. We can see that the optimal cache capacity increases with increasing γ_p . With the same cache capacity, ASE increases with γ_p . This is because the cache hit ratio p_h increases with γ_p as shown in (1) and those cached files own a higher popularity. The optimal AES with optimized cache capacity in $\gamma_p = 1$ over $\gamma_p = 0.2$ is about 300%.

While there are various kinds of memory technologies, we consider the three kinds that are most likely employed due to their higher power efficiencies and larger cache sizes. In Fig. 7(b), we show the numerical results of ASE versus cache capacity under different caching power coefficients. The cache power coefficients w_{ca} has an deep impact on the ASE. Low coefficient can improve the ASE over the optimized cache capacity. This is because when the w_{ca} is lower, more files can be cached with the same power overhead and the SBS cache hit ratio is improved. Then more files can be obtained from SBS directly and backhaul spectrum can be transferred to the access link.

F. APT and ASE

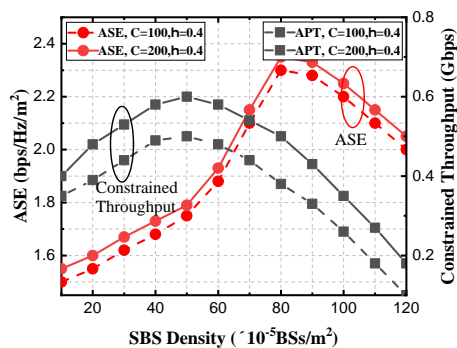


Fig. 8: APT(SINR requirement $\gamma_0 = 5dB$) and ASE under different SBS densities.

To reflect APT and ASE under different SBS densities, we give Fig. 8. From the Fig.8, we can see that both APT and ASE will increase with the increasing SBS density and then decrease. This is because when the when the BS density increases, LoS transmission exists with an increasingly higher probability than NLoS transmission. Therefore, the desired LoS signal from the associated BS is dominant. However, when the SBS becomes much denser, the interference power are LoS dominated and the data rate decrease. Compared with ASE, APT begins to decreases at a smaller

density. It is due to the fact that SINR requirement is more vulnerable to the LoS interference. When LoS interference increases with the increasing density, it is more difficult to satisfy the SINR requirement γ_0 of APT. When the cache capacity increases a little (e.e., from 100 to 200), both APT and ASE increase. This is because that, with more cache capacity, more files are sent directly from SBS and backhaul traffic is reduced. Then, the backhaul spectrum can be shifted to access and data rate is increased.

G. The Noise-limited Case and Interference-limited Case

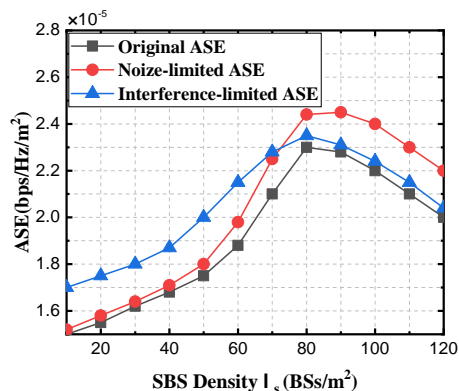


Fig. 9: Saved spectrum for access service under different cache capacities.

To verify the validity of the ASE approximations in noise-limited case and interference-limited case, we compare the numerical results of original ASE expression in (28) with those of noise-limited ASE (31) and of interference-limited ASE (34), respectively. Under the lower SBS density, the ASE expression (31) is a more effective upper bound of the original ASE expression in (28). That shows the simpler expression (31) captures the feature that lower density makes the mmWave signal more vulnerable to the noise. Besides, in the high density case, the ASE expression (34) is much closer to the original ASE expression in (28). These results show the effectiveness of the simpler ASE expression (31), which mainly focuses on the LoS based mmWave transmission.

VI. APPENDIX

A. The proof of Lemma 1

We first consider the event that the distance between the typical user and the nearest LoS SBS (LoS based file transmission between the typical user and the SBS) is r . In fact, the event

that is the joint of following two events: The first event is the nearest SBS of the typical user is located at distance r (Event 1) and the second event is the transmission path between the typical user and the serving SBS is an LoS path (Event 2). According to [40], the PDF of Event 1 with regard to r is given by $\exp(-\pi r^2 \lambda_s) \times 2\pi r \lambda_s$. The probability of Event 2 over distance r is $\mathcal{P}_L(r)$, so that we can get the PDF of the joint Event 1 and Event 2 as

$$f_{R_s}^L(r) = \mathcal{P}_L(r) \times \exp(-\pi r^2 \lambda_s) \times 2\pi r \lambda_s, \quad (37)$$

In a similar way, the PDF of the event that the distance between the typical user and the nearest NLoS SBS is r is

$$f_{R_s}^{\text{NL}}(r) = \mathcal{P}_{\text{NL}}(r) \times \exp(-\pi r^2 \lambda_s) \times 2\pi r \lambda_s, \quad (38)$$

The PDFs of the events that the distance between the user and the nearest LoS MBS (NLoS MBS) is r are

$$f_{R_m}^L(r) = \mathcal{P}_L(r) \times \exp(-\pi r^2 \lambda_m) \times 2\pi r \lambda_m, \quad (39)$$

$$f_{R_m}^{\text{NL}}(r) = \mathcal{P}_{\text{NL}}(r) \times \exp(-\pi r^2 \lambda_m) \times 2\pi r \lambda_m \quad (40)$$

B. The proof of Lemma 2

The typical user may associate with the SBS tier by either LoS channel or NLoS channel. We derive the probability of the first event that the user is associated with the SBS by the wireless LoS link. Such event has three cases: the interference from the NLoS SBS, the interference from the LoS MBS and the interference from the NLoS MBS. Therefore, the probability that the user obtain the desired LoS signal from the SBS is $F_s^L(r) = p_{ln}^{ss}(r)p_{ll}^{sm}(r)p_{ln}^{sm}(r)f_{R_s}^L(r)$ where

- 1) The user is associated with the LoS SBS and the interference is from NLoS SBS.

$$p_{ln}^{ss}(r) = \mathbb{P}[P_s^{tr} B_s h_s A_L r^{-\alpha_L} \geq P_s^{tr} B_s h_s A_{\text{NL}} r_s^{-\alpha_{\text{NL}}}] \quad (41)$$

$$= \mathbb{P}\left[r_s \geq \left(\frac{A_L}{A_{\text{NL}}}\right)^{\frac{-1}{\alpha_{\text{NL}}}} r^{\frac{\alpha_L}{\alpha_{\text{NL}}}}\right] = e^{-\lambda_s \pi \left[\left(\frac{A_L}{A_{\text{NL}}}\right)^{\frac{-1}{\alpha_{\text{NL}}}} r^{\frac{\alpha_L}{\alpha_{\text{NL}}}}\right]^2} \quad (42)$$

where the last step is based on the derivation in [40].

- 2) The user is associated with the LoS SBS and the interference is from LoS MBS.

$$p_{ll}^{sm}(r) = \mathbb{P}[P_s^{tr} h_s A_L r^{-\alpha_L} \geq P_m^{tr} B_m h_m A_L r_m^{-\alpha_L}] \quad (43)$$

$$= \mathbb{P}\left[r_m \geq \left(\frac{P_s^{tr} B_s h_s}{P_m^{tr} B_m h_m}\right)^{\frac{-1}{\alpha_L}} r\right] = e^{-\lambda_m \pi \left[\left(\frac{P_s^{tr} B_s h_s}{P_m^{tr} B_m h_m}\right)^{\frac{-1}{\alpha_L}} r\right]^2} \quad (44)$$

3) The user is associated with the LoS SBS and the interference is from NLoS MBS.

$$p_{ln}^{sm}(r) = \mathbb{P}[P_s^{tr} B_s h_s A_L r^{-\alpha_L} \geq P_m^{tr} B_m h_m A_{NL} r_m^{-\alpha_{NL}}] \quad (45)$$

$$= \mathbb{P}\left[r_m \geq \left(\frac{P_s^{tr} B_s h_s A_L}{P_m^{tr} B_m h_m A_{NL}}\right)^{\frac{-1}{\alpha_{NL}}} r^{\frac{\alpha_L}{\alpha_{NL}}}\right] = e^{-\lambda_m \pi \left[\left(\frac{P_s^{tr} B_s h_s A_L}{P_m^{tr} B_m h_m A_{NL}}\right)^{\frac{-1}{\alpha_{NL}}} r^{\frac{\alpha_L}{\alpha_{NL}}}\right]^2} \quad (46)$$

Then, the probability that the user obtain the desired NLoS signal from the SBS is $F_s^{NL}(r) = p_{nl}^{ss}(r) p_{nl}^{sm}(r) p_{nn}^{sm}(r) f_{R_s}^{NL}(r)$ where

1) The user is associated with the NLoS SBS and the interference is from LoS SBS.

$$p_{nl}^{ss}(r) = P[P_s^{tr} B_s h_s A_{NL} r^{-\alpha_{NL}} \geq P_s^{tr} B_s h_s A_L r_s^{-\alpha_L}] = e^{-\lambda_s \pi \left[\left(\frac{A_{NL}}{A_L}\right)^{\frac{-1}{\alpha_L}} r^{\frac{\alpha_{NL}}{\alpha_L}}\right]^2} \quad (47)$$

2) The user is associated with the NLoS SBS and the interference is from LoS MBS.

$$p_{nl}^{sm}(r) = P[P_s^{tr} B_s h_s A_{NL} r^{-\alpha_{NL}} \geq P_m^{tr} B_m h_m A_L r_m^{-\alpha_L}] = e^{-\lambda_m \pi \left[\left(\frac{P_s^{tr} B_s h_s A_{NL}}{P_m^{tr} B_m h_m A_L}\right)^{\frac{-1}{\alpha_L}} r^{\frac{\alpha_{NL}}{\alpha_L}}\right]^2} \quad (48)$$

3) The user is associated with the NLoS SBS and the interference is from NLoS MBS.

$$p_{nn}^{sm}(r) = P[P_s^{tr} B_s h_s A_{NL} r^{-\alpha_{NL}} \geq P_m^{tr} B_m h_m A_{NL} r_m^{-\alpha_{NL}}] = e^{-\lambda_m \pi \left[\left(\frac{P_s^{tr} B_s h_s}{P_m^{tr} B_m h_m}\right)^{\frac{-1}{\alpha_{NL}}} r\right]^2} \quad (49)$$

Then, the probability that the user obtain the desired LoS signal from the MBS is $F_m^L(r) = p_{ln}^{mm}(r) p_{ll}^{ms}(r) p_{ln}^{sm}(r) f_{R_m}^L(r)$ where

1) The user is associated with the LoS MBS and the interference is from NLoS MBS.

$$p_{ln}^{mm}(r) = P[P_m^{tr} B_m h_m A_L r^{-\alpha_L} \geq P_m^{tr} B_m h_m A_{NL} r_m^{-\alpha_{NL}}] = e^{-\lambda_m \pi \left[\left(\frac{A_L}{A_{NL}}\right)^{\frac{-1}{\alpha_{NL}}} r^{\frac{\alpha_L}{\alpha_{NL}}}\right]^2} \quad (50)$$

2) The user is associated with the LoS MBS and the interference is from LoS SBS.

$$p_{ll}^{ms}(r) = p[P_m^{tr} B_m h_m A_L r^{-\alpha_L} \geq P_s^{tr} B_s h_s A_L r_s^{-\alpha_L}] = e^{-\lambda_s \pi \left[\left(\frac{P_m^{tr} B_m h_m}{P_s^{tr} B_s h_s}\right)^{\frac{-1}{\alpha_L}} r\right]^2} \quad (51)$$

3) The user is associated with the LoS MBS and the interference is from NLoS SBS.

$$p_{ln}^{sm}(r) = P[P_m^{tr} B_m h_m A_L r^{-\alpha_L} \geq P_s^{tr} B_s h_s A_{NL} r_s^{-\alpha_{NL}}] = e^{-\lambda_s \pi \left[\left(\frac{P_m^{tr} B_m h_m A_L}{P_s^{tr} B_s h_s A_{NL}}\right)^{\frac{-1}{\alpha_{NL}}} r^{\frac{\alpha_L}{\alpha_{NL}}}\right]^2} \quad (52)$$

Then, the probability that the user obtain the desired NLoS signal from the MBS is $F_m^{NL}(r) = p_{nl}^{mm}(r) p_{nl}^{ms}(r) p_{nn}^{ms}(r) f_{R_m}^{NL}(r)$ where

1) The user is associated with the NLoS MBS and the interference is from LoS MBS.

$$p_{nl}^{mm}(r) = P[P_m^{tr} B_m h_m A_{NL} r^{-\alpha_{NL}} \geq P_m^{tr} B_m h_m A_L r_m^{-\alpha_L}] = e^{-\lambda_m \pi \left[\left(\frac{A_{NL}}{A_L} \right)^{\frac{-1}{\alpha_L}} r^{\frac{\alpha_{NL}}{\alpha_L}} \right]^2} \quad (53)$$

2) The user is associated with the NLoS MBS and the interference is from LoS SBS.

$$p_{nl}^{ms}(r) = P[P_m^{tr} B_m h_m A_{NL} r^{-\alpha_{NL}} \geq P_s^{tr} B_s h_s A_L r_s^{-\alpha_L}] = e^{-\lambda_s \pi \left[\left(\frac{P_m^{tr} B_m h_m A_{NL}}{P_s^{tr} B_s h_s A_L} \right)^{\frac{-1}{\alpha_L}} r^{\frac{\alpha_{NL}}{\alpha_L}} \right]^2} \quad (54)$$

3) The user is associated with the NLoS MBS and the interference is from NLoS SBS.

$$p_{nn}^{ms}(r) = P[P_m^{tr} B_m h_m A_{NL} r^{-\alpha_{NL}} \geq P_s^{tr} B_s h_s A_{NL} r_s^{-\alpha_{NL}}] = e^{-\lambda_s \pi \left[\left(\frac{P_m^{tr} B_m h_m}{P_s^{tr} B_s h_s} \right)^{\frac{-1}{\alpha_{NL}}} r \right]^2} \quad (55)$$

The probability that SBS obtains the desired LoS signal from MBS is $F_{bh}^L(r) = p_{ln}^{bh}(r) f_{R_{bh}}^L(r)$ where $p_{ln}^{bh}(r) = P[P_m^{tr} B_m h_m A_L r^{-\alpha_L} \geq P_m^{tr} B_m h_m A_{NL} r_{bh}^{-\alpha_{NL}}] = e^{-\lambda_m \pi \left[\left(\frac{A_L}{A_{NL}} \right)^{\frac{-1}{\alpha_{NL}}} r^{\frac{\alpha_L}{\alpha_{NL}}} \right]^2}$ is the probability that the SBS is associated with the LoS MBS and the interference is from NLoS MBS.

The probability that SBS obtains the desired NLoS signal from MBS is $F_{bh}^{NL}(r) = p_{nl}^{bh}(r) f_{R_{bh}}^{NL}(r)$ where $p_{nl}^{bh}(r) = P[P_m^{tr} B_m h_m A_{NL} r^{-\alpha_{NL}} \geq P_m^{tr} B_m h_m A_L r_{bh}^{-\alpha_L}] = e^{-\lambda_m \pi \left[\left(\frac{A_{NL}}{A_L} \right)^{\frac{-1}{\alpha_L}} r^{\frac{\alpha_{NL}}{\alpha_L}} \right]^2}$ is the probability that the SBS is associated with the NLoS MBS and the interference is from LoS MBS.

C. Proof of Proposition 1

Then we first focus on the SINR distribution of a user covered by SBS:

$$P_s^{cov}(\gamma) = P_{s,L}^{cov}(\gamma) + P_{s,NL}^{cov}(\gamma) \quad (56)$$

where the SINR distribution of a user covered by LoS SBS:

$$P_{s,L}^{cov}(\gamma) = \mathbb{E}_r [\mathbb{P} [\text{SINR}_s^L(r) \geq \gamma]] = \int_0^\infty \mathbb{P} [\text{SINR}_s^L(r) > \gamma] F_s^L(r) dr \quad (57)$$

and the SINR distribution of a user covered by NLoS SBS:

$$P_{s,NL}^{cov}(\gamma) = \mathbb{E}_r [\mathbb{P} [\text{SINR}_s^{NL}(r) \geq \gamma]] = \int_0^\infty \mathbb{P} [\text{SINR}_s^{NL}(r) > \gamma] F_s^{NL}(r) dr \quad (58)$$

where γ is the threshold for successful demodulation and decoding at the receiver. $\mathbb{P} [\text{SINR}_s^L(r) \geq \gamma]$ means the probability of the event that the SINR of the user covered by SBS is over γ via the LoS path at distance r :

$$\begin{aligned} \mathbb{P} [\text{SINR}_s^L(r) \geq \gamma] &= \mathbb{P} \left[\frac{P_s^{tr} B_s A_L r^{-\alpha_L}}{I_s + I_m + N_0} \geq \gamma \right] \\ &= \mathbb{P} \left[h_m \geq \frac{\gamma (I_s + I_m + N_0)}{P_s^{tr} B_s A_L r^{-\alpha_L}} \right] \stackrel{(a)}{=} \exp \left(\frac{-\gamma N_0}{P_s^{tr} B_s A_L r^{-\alpha_L}} \right) \mathcal{L}_{I_{s,m}}^L (\gamma r^{\alpha_L}) \end{aligned} \quad (59)$$

Besides, $\mathbb{P} [\text{SINR}_s^{\text{NL}}(r) \geq \gamma]$ means the probability of the event that the SINR of the user covered by SBS is over γ via the NLoS path at distance r :

$$\begin{aligned} \mathbb{P} [\text{SINR}_s^{\text{NL}}(r) \geq \gamma] &= \mathbb{P} \left[\frac{P_s^{tr} B_s G_s A_L r^{-\alpha_{\text{NL}}}}{I_s + I_m + N_0} \geq \gamma \right] \\ &= \mathbb{P} \left[h_{m0} \geq \frac{\gamma (I_s + I_m + N_0)}{P_s^{tr} B_s A_{\text{NL}} r^{-\alpha_{\text{NL}}}} \right] \stackrel{(a)}{=} \exp \left(\frac{-\gamma N_0}{P_s^{tr} B_s h_s A_{\text{NL}} r^{-\alpha_{\text{NL}}}} \right) \mathcal{L}_{I_{s,m}}^{\text{NL}} (\gamma r^{\alpha_{\text{NL}}}) \end{aligned} \quad (60)$$

where (a) follows from small fading $h \sim \exp(1)$. Here the Rayleigh fading is considered. $\mathcal{L}_{I_{s,m}}$ is the Laplace transform of the cumulative interference from the SBS tier.

$$\begin{aligned} &\mathcal{L}_{I_{s,m}}^L (\gamma r^{\alpha_L}) \\ &\stackrel{(b)}{=} \exp \left(-2\pi\lambda_s \left(\int_r^\infty \frac{\mathcal{P}_L(u)u}{1 + \frac{P_s^{tr} B_s h_s A_L r^{-\alpha_L}}{\gamma P_s^{tr} B_s h_s A_L u^{-\alpha_L}}} du + \int_{\left(\frac{A_L}{A_{\text{NL}}}\right)^{\frac{-1}{\alpha_{\text{NL}}}} r^{\frac{\alpha_L}{\alpha_{\text{NL}}}}}^\infty \frac{\mathcal{P}_{\text{NL}}(u)u}{1 + \frac{P_s^{tr} B_s h_s A_L r^{-\alpha_L}}{\gamma P_s^{tr} B_s h_s A_{\text{NL}} u^{-\alpha_{\text{NL}}}}} du \right) \right) \\ &\times \exp \left(-2\pi\lambda_m \left(\int_{(d_1)^{\frac{-1}{\alpha_L}} r}^\infty \frac{\mathcal{P}_L(u)u}{1 + \frac{P_s^{tr} B_s h_s A_L r^{-\alpha_L}}{\gamma P_m^{tr} B_m h_m A_L u^{-\alpha_L}}} du + \int_{(d_2)^{\frac{-1}{\alpha_{\text{NL}}}} r^{\frac{\alpha_L}{\alpha_{\text{NL}}}}}^\infty \frac{\mathcal{P}_{\text{NL}}(u)u}{1 + \frac{P_s^{tr} B_s h_s A_L r^{-\alpha_L}}{\gamma P_m^{tr} B_m h_m A_L u^{-\alpha_{\text{NL}}}}} du \right) \right) \end{aligned} \quad (61)$$

where step (b) is based on [40]. $d_1 = \frac{P_s^{tr} B_s h_s}{P_m^{tr} B_m h_m}$ and $d_2 = \frac{P_s^{tr} B_s h_s A_L}{P_m^{tr} B_m h_m A_{\text{NL}}}$. Following the same logic, $\mathcal{L}_{I_{s,m}}^{\text{NL}} (\gamma r^{\alpha_{\text{NL}}})$, $\mathcal{L}_{I'_{s,m}}^L (\gamma r^{\alpha_L})$, $\mathcal{L}_{I'_{s,m}}^{\text{NL}} (\gamma r^{\alpha_{\text{NL}}})$, $\mathcal{L}_{I_{bh}}^L (\gamma r^{\alpha_L})$, $\mathcal{L}_{I_{bh}}^{\text{NL}} (\gamma r^{\alpha_{\text{NL}}})$ can be also obtained.

In the next, we focus on the SINR distribution of a user covered by MBS :

$$\begin{aligned} P_m^{\text{cov}} &= P_{m,L}^{\text{cov}}(\gamma) + P_{m,\text{NL}}^{\text{cov}}(\gamma) = \mathbb{E}_r [\mathbb{P} [\text{SINR}_m^L(r) \geq \gamma]] + \mathbb{E}_r [\mathbb{P} [\text{SINR}_m^{\text{NL}}(r) \geq \gamma]] \\ &= \int_0^\infty \mathbb{P} [\text{SINR}_m^L(r) > \gamma] F_m^L(r) dr + \int_0^\infty \mathbb{P} [\text{SINR}_m^{\text{NL}}(r) > \gamma] F_m^{\text{NL}}(r) dr \end{aligned}$$

where $\mathbb{P} [\text{SINR}_m^L(r) \geq \gamma] = \exp \left(\frac{-\gamma N_0}{P_m^{tr} B_m A_L r^{-\alpha_L}} \right) \mathcal{L}_{I'_{s,m}}^L (\gamma r^{\alpha_L})$ and $\mathbb{P} [\text{SINR}_m^{\text{NL}}(r) \geq \gamma]$
 $= \exp \left(\frac{-\gamma N_0}{P_m^{tr} B_m g_m A_{\text{NL}} r^{-\alpha_{\text{NL}}}} \right) \mathcal{L}_{I'_{s,m}}^{\text{NL}} (\gamma r^{\alpha_{\text{NL}}})$

Considering SBS is also covered by MBS via the wireless backhaul link, we focus on the SINR distribution of a SBS is covered by MBS:

$$\begin{aligned}
P_{bh}^{cov}(\gamma) &= P_{bh,L}^{cov}(\gamma) + P_{bh,NL}^{cov}(\gamma) \\
&= \mathbb{E}_r [\mathbb{P} [\text{SINR}_{bh}^L(r) \geq \gamma]] + \mathbb{E}_r [\mathbb{P} [\text{SINR}_{bh}^{NL}(r) \geq \gamma]] \\
&= \int_0^\infty \mathbb{P} [\text{SINR}_{bh}^L(r) > \gamma] F_{bh}^L(r) dr + \int_0^\infty \mathbb{P} [\text{SINR}_{bh}^{NL}(r) > \gamma] F_{bh}^{NL}(r) dr
\end{aligned} \tag{62}$$

where $\mathbb{P} [\text{SINR}_{bh}^L(r) \geq \gamma] = \exp\left(\frac{-\gamma N_0}{P_m^{tr} B_m g_m A_L r^{-\alpha_L}}\right) \mathcal{L}_{I_{bh}}^L(\gamma r^{\alpha_L})$ and $\mathbb{P} [\text{SINR}_{bh}^{NL}(r) \geq \gamma]$
 $= \exp\left(\frac{-\gamma N_0}{P_m^{tr} B_m g_m A_{NL} r^{-\alpha_{NL}}}\right) \mathcal{L}_{I_{bh}}^{NL}(\gamma r^{\alpha_{NL}})$

D. Proof of Proposition 2

For the user associating with SBS tier, the user spectral efficiency distribution is $\mathbb{P}[R_s > \rho]$ where R_s denotes the spectral efficiency of a typical user associating a serving SBS and ρ is the spectral efficiency requirement. When a user associated with the SBS is requesting files, the cached files will be delivered by the SBS directly and the uncached files will be delivered to the user through the wireless backhaul link and wireless access link. Therefore, the spectral efficiency of the user associated with serving SBS is not only limited by the wireless link capacity and backhaul link capacity, but also is related with the cache hit ratio p_h . Namely, $R_s = \min\{\eta \log_2(1 + \text{SINR}_s(r)), \frac{1-\eta}{1-p_h} \log_2(1 + \text{SINR}_{bh}(r))\}$. However, since the transmission of the wireless access link and the wireless backhaul link is either LoS or NLoS, the below four cases of $\mathbb{P}[R_s > \rho]$ are analyzed:

- Files are delivered by both LoS based wireless access link and the wireless backhaul link.

$$\begin{aligned}
\mathbb{P}[R_{s,1} > \rho] & \\
&= \mathbb{P}\left[\min\{\eta \log_2(1 + \text{SINR}_s^L(r)), \frac{1-\eta}{1-p_h} \log_2(1 + \text{SINR}_{bh}^L(r))\} \geq \rho\right] \\
&= \mathbb{P}\left[\eta \log_2(1 + \text{SINR}_s^L(r)) > \rho\right] \times \mathbb{P}\left[(1-\eta) \log_2(1 + \text{SINR}_{bh}^L(r)) > (1-p_h)\rho\right] \\
&= \mathbb{P}\left[\text{SINR}_s^L(r) \geq 2^{\frac{\rho}{\eta}} - 1\right] \times \mathbb{P}\left[\text{SINR}_{bh}^L(r) \geq 2^{\frac{(1-p_h)\rho}{(1-\eta)}} - 1\right] \\
&= \mathbb{P}_{s,L}^{cov}\left(2^{\frac{\rho}{\eta}} - 1 | r_s\right) \times \mathbb{P}_{bh,L}^{cov}\left(2^{\frac{(1-p_h)\rho}{(1-\eta)}} - 1 | r_{bh}\right)
\end{aligned} \tag{63}$$

- Files are delivered by LoS based wireless access link and NLoS based wireless backhaul.

$$\mathbb{P}[R_{s,2} > \rho] = \mathbb{P}_{s,L}^{cov}\left(2^{\frac{\rho}{\eta}} - 1 | r_s\right) \times \mathbb{P}_{bh,NL}^{cov}\left(2^{\frac{(1-p_h)\rho}{(1-\eta)}} - 1 | r_{bh}\right) \tag{64}$$

- Files are delivered by NLoS based wireless access link and LoS based wireless backhaul.

$$\mathbb{P}[R_{s,3} > \rho] = \mathbb{P}_{s,\text{NL}}^{\text{cov}}(2^{\frac{\rho}{\eta}} - 1|r_s) \times \mathbb{P}_{bh,L}^{\text{cov}}(2^{\frac{(1-p_h)\rho}{(1-\eta)}} - 1|r_{bh}) \quad (65)$$

- Files are delivered by NLoS based wireless access link and NLoS based wireless backhaul.

$$\mathbb{P}[R_{s,4} > \rho] = \mathbb{P}_{s,\text{NL}}^{\text{cov}}(2^{\frac{\rho}{\eta}} - 1|r_s) \times \mathbb{P}_{bh,\text{NL}}^{\text{cov}}(2^{\frac{(1-p_h)\rho}{(1-\eta)}} - 1|r_{bh}) \quad (66)$$

where $\mathbb{P}_{s,L}^{\text{cov}}(\cdot)$ and $\mathbb{P}_{s,\text{NL}}^{\text{cov}}(\cdot)$ are the SINR distributions of the user covered by LoS SBS and NLoS SBS, respectively. $\mathbb{P}_{m,L}^{\text{cov}}(\cdot)$ and $\mathbb{P}_{m,\text{NL}}^{\text{cov}}(\cdot)$ are the SINR distributions of SBS covered by LoS MBS and NLoS MBS, respectively (in Proposition 1).

Following the same logic, for the user associated with the MBS, the spectral efficiency distribution is divided into two cases:

- The access link between the user and the MBS is LoS:

$$\mathbb{P}[R_{m,1} > \rho] = \mathbb{P}[\eta \log_2(1 + \text{SINR}_m^L(r)) > \rho] = \mathbb{P}[\text{SINR}_m^L(r) \geq 2^{\frac{\rho}{\eta}} - 1] = \mathbb{P}_{m,L}^{\text{cov}}(2^{\frac{\rho}{\eta}} - 1|r_m) \quad (67)$$

- The access link between the user and the MBS is NLoS:

$$\mathbb{P}[R_{m,2} > \rho] = \mathbb{P}[\text{SINR}_m^{\text{NL}}(r) \geq 2^{\frac{\rho}{\eta}} - 1] = \mathbb{P}_{m,\text{NL}}^{\text{cov}}(2^{\frac{\rho}{\eta}} - 1|r_m) \quad (68)$$

where $\mathbb{P}_{s,L}^{\text{cov}}(\cdot)$ and $\mathbb{P}_{s,\text{NL}}^{\text{cov}}(\cdot)$ are the SINR distributions of the user covered by LoS MBS and NLoS MBS, respectively (in Proposition 1).

E. The proof of Proposition 3

when the density of SBS is higher (i.e., $\lambda_s \rightarrow \infty$), the SBS will become more closer to the user. All the transmission signal from SBS will be transmitted in an LoS channel to the user (i.e., $\mathcal{P}_L(r) = 1$). That means the NLoS transmission of SBS is neglected. Besides, the original $\bar{\mathcal{L}}_{I_{s,m}}^L$ in the general ASE of SBS (29) will be approximated as:

$$\bar{\mathcal{L}}_{I_{s,m}}^{\text{L,int}}(\gamma r^{\alpha_L}) \approx \exp\left(-2\pi\lambda_s \int_r^\infty \frac{u}{1 + \frac{r^{-\alpha_L}}{\gamma u^{-\alpha_L}}} du - 2\pi\lambda_m \int\left(\frac{P_s^{\text{tr}}}{P_s^{\text{tr}}}\right)^{\frac{1}{\alpha_L}} r \frac{u}{1 + \frac{P_s^{\text{tr}} B_s h_s A_L r^{-\alpha_L}}{\gamma P_m^{\text{tr}} B_m h_m A_L u^{-\alpha_L}}} du\right) \quad (69)$$

And the original $\bar{\mathcal{L}}_{I_{s,m}}^{\text{NL}}$ in the general ASE of SBS (29) will be approximated to zero in the interference-limited case.

With the above analysis, based on the general ASE of SBS in (29), the ASE of SBS in the interference-limited case is obtained and given in the Proposition 3.

REFERENCES

- [1] C. Dehos, J. L. González, A. De Domenico, D. Kténas, and L. Dussopt, "Millimeter-wave Access and Backhauling: The Solution to the Exponential Data Traffic Increase in 5G Mobile Communications Systems?" *IEEE Commun. Mag.*, vol. 52, no. 9, pp. 8895, Sep. 2014.
- [2] R. Taori and A. Sridharan, "Point-to-Multipoint in-band Mmwave Backhaul for 5G Networks," *IEEE Commun. Mag.*, vol. 53, no. 1, pp. 195-201, Jan. 2015.
- [3] R. J. Weiler et al., "Enabling 5G Backhaul and Access with Millimeter-waves," in *Proc. IEEE EuCNC 2014*, Bologna, 2014, pp. 1-5.
- [4] NR; Study on Integrated Access and Backhaul, document 3GPP TR 38.874, 2017.
- [5] A. AlAmmouri, J. G. Andrews and F. Baccelli, "A Unified Asymptotic Analysis of Area Spectral Efficiency in Ultradense Cellular Networks," *IEEE Trans. Inf. Theory*, vol. 65, no. 2, pp. 1236-1248, Feb. 2019.
- [6] X. Zhang and J. G. Andrews, "Downlink Cellular Network Analysis With Multi-Slope Path Loss Models," *IEEE Trans. Commun.*, vol. 63, no. 5, pp. 1881-1894, May 2015.
- [7] I. Atzeni, J. Arnau and M. Kountouris, "Downlink Cellular Network Analysis With LOS/NLOS Propagation and Elevated Base Stations," *IEEE Trans. Wireless Commun.*, vol. 17, no. 1, pp. 142-156, Jan. 2018.
- [8] M. Ding, D. Lopez-Perez, G. Mao, P. Wang and Z. Lin, "Will the Area Spectral Efficiency Monotonically Grow as Small Cells Go Dense?," *Proc. IEEE GLOBECOM*, San Diego, CA, 2015, pp. 1-7.
- [9] X. Wang, E. Turgut and M. C. Gursoy, "Coverage in Downlink Heterogeneous mmWave Cellular Networks With User-Centric Small Cell Deployment," *IEEE Trans. Veh. Technol.*, vol. 68, no. 4, pp. 3513-3533, April 2019.
- [10] W. Yi, Y. Liu and A. Nallanathan, "Modeling and Analysis of D2D Millimeter-Wave Networks With Poisson Cluster Processes," *IEEE Trans. Commun.*, vol. 65, no. 12, pp. 5574-5588, Dec. 2017.
- [11] S. Hur, T. Kim, D. J. Love, J. V. Krogmeier, T. A. Thomas and A. Ghosh, "Millimeter Wave Beamforming for Wireless Backhaul and Access in Small Cell Networks," *IEEE Trans. Commun.*, vol. 61, no. 10, pp. 4391-4403, Oct. 2013.
- [12] Z. Shi, Y. Wang, L. Huang and T. Wang, "Dynamic Resource Allocation in MmWave Unified Access and Backhaul Network," *Proc. PIMRC*, Hong Kong, 2015, pp. 2260-2264.
- [13] C. Saha, M. Afshang and H. S. Dhillon, "Bandwidth Partitioning and Downlink Analysis in Millimeter Wave Integrated Access and Backhaul for 5G," *IEEE Trans. Wireless Commun.*, vol. 17, no. 12, pp. 8195-8210, Dec. 2018.
- [14] D. Liu, B. Chen, C. Yang and A. F. Molisch, "Caching at the Wireless Edge: Design Aspects, Challenges, and Future Directions," *IEEE Commun. Mag.*, vol. 54, no. 9, pp. 22-28, 2016.
- [15] M. Tao, E. Chen, H. Zhou and W. Yu, "Content-centric Sparse Multicast Beamforming for Cache-enabled Cloud RAN," *IEEE Trans. Wireless Commun.*, vol. 15, no. 9, pp. 6118-6131, Sept. 2016.
- [16] X. Xu and M. Tao, "Modeling, Analysis, and Optimization of Coded Caching in Small-cell Networks," *IEEE Trans. Commun.*, vol. 65, no. 8, pp. 3415-3428, Aug. 2017.
- [17] Y. Chiang and W. Liao, "ENCORE: An Energy-aware Multicell Cooperation in Heterogeneous Networks with Content Caching," *Proc. IEEE INFOCOM*, San Francisco, CA, 2016, pp. 1-9.
- [18] D. Liu and C. Yang, "Energy Efficiency of Downlink Networks With Caching at Base Stations," *IEEE J. Sel. Areas Commun.*, vol. 34, no. 4, pp. 907-922, April 2016.
- [19] F. Gabry, V. Bioglio and I. Land, "On Energy-Efficient Edge Caching in Heterogeneous Networks," *IEEE J. Sel. Areas Commun.*, vol. 34, no. 12, pp. 3288-3298, Dec. 2016.
- [20] H. ElSawy, E. Hossain, and M. Haenggi, "Stochastic geometry for modeling, analysis, and design of multi-tier and cognitive cellular wireless networks: A survey," *IEEE Commun. Surveys Tuts.*, vol. 15, no. 3, pp. 9961019, Jun. 2013.

- [21] J. Llorca et al., “Dynamic In-network Caching for Energy Efficient Content Delivery,” in *Proc. IEEE INFOCOM*, 2013, pp. 245249.
- [22] K. Shanmugam, N. Golrezaei, A. G. Dimakis, A. F. Molisch and G. Caire, “FemtoCaching: Wireless Content Delivery Through Distributed Caching Helpers,” *IEEE Trans. Inf. Theory*, vol. 59, no. 12, pp. 8402-8413, Dec. 2013.
- [23] P. Gill, M. Arlitt, Z. Li, and A. Mahanti, “YouTube Traffic Characterization: A View from the Edge,” in *Proc. ACM IMC*, San Diego, CA, Oct. 2007.
- [24] L. Breslau, P. Cao, L. Fan, G. Phillips, and S. Shenker, “Web Caching and Zipf-like Distributions: Evidence and Implications,” in *Proc. IEEE INFOCOM*, 1999, pp. 126134.
- [25] M. Cha, P. Rodriguez, J. Crowcroft, S. Moon, and X. Amatriain, “Atching Television over An IP Network,” in *Proc. ACM SIGCOMM IMC*, 2008, pp. 126134.
- [26] G. Quer, I. Pappalardo, B. D. Rao and M. Zorzi, “Proactive Caching Strategies in Heterogeneous Networks With Deviceto-Device Communications,” *IEEE Trans. Wireless Commun.*, vol. 17, no. 8, pp. 5270-5281, Aug. 2018.
- [27] T. Bai, R. Vaze, and R. Heath, “Analysis of blockage effects on urban cellular networks,” *IEEE Trans. Wireless Commun.*, vol. 13, no. 9, pp. 50705083, Sep. 2014.
- [28] C. Shuguang, A. J. Goldsmith, and A. Bahai, “Energy-Constrained Modulation Optimization,” *IEEE Trans. Wireless Commun.*, vol. 4, no. 5, pp. 23492360, Sep 2005.
- [29] A. K. Gupta, J. G. Andrews and R. W. Heath, “On the Feasibility of Sharing Spectrum Licenses in mmWave Cellular Systems,” *IEEE Trans. Commun.*, vol. 64, no. 9, pp. 3981-3995, Sept. 2016.
- [30] S. Singh, M. N. Kulkarni, A. Ghosh, and J. G. Andrews, “Tractable Model for Rate in Self-backhauled Millimeter Wave Cellular Networks,” *IEEE J. Sel. Areas Commun.*, vol. 33, no. 10, pp. 21962211, Oct. 2015.
- [31] J. G. Andrews, T. Bai, M. N. Kulkarni, A. Alkhateeb, A. K. Gupta, and R. W. Heath, Jr., “Modeling and Analyzing Millimeter Wave Cellular systems,” *IEEE Trans. Commun.*, vol. 65, no. 1, pp. 403430, Jan. 2017.
- [32] E. Turgut and M. C. Gursoy, “Coverage in Heterogeneous Downlink Millimeter Wave Cellular Networks,” *IEEE Trans. Commun.*, vol. 65, no. 10, pp. 4463-4477, Oct. 2017.
- [33] B. Yang, G. Mao, M. Ding, X. Ge and X. Tao, “Dense Small Cell Networks: From Noise-Limited to Dense Interference-Limited,” *IEEE Trans. Wireless Commun.*, vol. 67, no. 5, pp. 4262-4277, May 2018.
- [34] B. Yang, G. Mao, M. Ding, X. Ge and X. Tao, “Dense Small Cell Networks: From Noise-Limited to Dense Interference-Limited,” *IEEE Trans. Veh. Technol.*, vol. 67, no. 5, pp. 4262-4277, May 2018.
- [35] T. Bai and R. W. Heath, “Coverage and Rate Analysis for Millimeter-Wave Cellular Networks,” *IEEE Trans. Wireless Commun.*, vol. 14, no. 2, pp. 1100-1114, Feb. 2015.
- [36] 3GPP TR 36.942 V12.0.0, “Radio Frequency (RF) System Scenarios (Release 12),” Sep. 2010.
- [37] M. Ding, P. Wang, D. López-Pérez, G. Mao and Z. Lin, “Performance Impact of LoS and NLoS Transmissions in Dense Cellular Networks,” *IEEE Trans. Wireless Commun.*, vol. 15, no. 3, pp. 2365-2380, March 2016.
- [38] M. Peng, K. Zhang, J. Jiang, J. Wang and W. Wang, “Energy-Efficient Resource Assignment and Power Allocation in Heterogeneous Cloud Radio Access Networks,” *IEEE Trans. Veh. Technol.*, vol. 64, no. 11, pp. 5275-5287, Nov. 2015.
- [39] C. Liu and K. L. Fong, “Fundamentals of the Downlink Green Coverage and Energy Efficiency in Heterogeneous Networks,” *IEEE J. Sel. Areas Commun.*, vol. 34, no. 12, pp. 3271-3287, Dec. 2016.
- [40] J. G. Andrews, F. Baccelli, and R. K. Ganti, “A Tractable Approach to Coverage and Rate in Cellular Networks,” *IEEE Trans. Commun.*, vol. 59, no. 11, pp. 31223134, 2011.